2000-01-0335

# Ultra-lightweight Aluminum Foam Materials for Automotive Applications

**T. Dennis Claar and Chin-Jye Yu**
Fraunhofer USA Center - Delaware, Newark, Delaware, USA

**Ian Hall**
University of Delaware, Newark, Delaware, USA

**John Banhart and Joachim Baumeister**
Fraunhofer Institute for Applied Materials Research, Bremen, Germany

**Wolfgang Seeliger**
Karmann GmbH, Osnabrück, Germany



## ABSTRACT

Ultra-lightweight metal foams are an emerging class of new engineering materials that can be tailored to have a very attractive combination of properties. Aluminum foams produced by Fraunhofer's powder metallurgy process show significant promise as multi-functional materials for a broad range of transportation applications. Their light weight and very high specific stiffness offer significant potential for vehicle weight reduction. The high energy absorption capabilities of aluminum foams can provide improved crash energy management. The range of materials properties that can be achieved using aluminum foams in various configurations and in combination with other structural materials are discussed. Current and potential future applications of aluminum foams in autos, trucks, and military vehicles for weight reduction, increased fuel efficiency, and improved mobility are also described.

## INTRODUCTION

Metal foams with high levels of controlled porosity are an emerging class of ultra-lightweight materials that are receiving increased attention for both commercial and military applications (1,2). Aluminum metal foam materials, which can be fabricated into a variety of functional geometries, offer significant performance advantages for weight-sensitive applications. Metal foams exhibit high stiffness-to-weight and strength-to-weight ratios, and thus offer potential weight savings. They also have the ability to absorb high amounts of energy during compressive deformation for efficient crash energy management.

Fraunhofer-Gesellschaft, at its Institute for Applied Materials Research (IFAM) in Bremen, Germany, has developed and patented a process for producing metal foam materials and shapes, based on a powder metallurgy (P/M) route (3,4). Further development and application of aluminum foam technology is being conducted by Fraunhofer IFAM and the Fraunhofer USA Center – Delaware in collaboration with industrial and university partners. This method allows for low cost and direct net-shaped fabrication of foamed parts with a relatively homogeneous pore structure. Using the powder metallurgical production method, it is possible to produce foams from a variety of metal and alloy compositions. Various foam geometries are also possible, including net shaped complex 3-D molded parts, metal foam sandwich panels, and metal foam-filled tubes and structural shapes. Metallic foams fabricated by this approach exhibit a closed-cell microstructure with higher mechanical strength than open-cell foams. This type of microstructure is particularly attractive for applications requiring reduced weight and efficient energy absorption capabilities.

## P/M PROCESS FOR PRODUCING METAL FOAMS

### DESCRIPTION OF METAL FOAM PROCESS

The Fraunhofer P/M process for producing metal foams is shown schematically in Figure 1. The overall process is based on blending metal powders with a foaming agent, compacting the powder mixture to high density, and then heating the compact to near the melting point of the metal. The process starts with mixing metal powders (either pre-alloyed metal powders or blends of

elemental powders) with a small amount of foaming agent (if metal hydrides are used, a content of less than 1% is sufficient in most cases). After the foaming agent is uniformly distributed within the matrix powders, the mixture is compacted to yield a dense, semi-finished product without any residual open porosity. Typical examples of such compaction methods include uniaxial pressing, extrusion, and powder rolling. Further shaping of the foamable material can be achieved through subsequent metalworking processes such as rolling, swaging or extrusion. Examples of the semi-finished products include billets, plates, and rods.

Following the powder consolidation and metalworking steps, the foamable precursor material is heated to the process temperature. At this stage, the foaming agent decomposes, forming a gas that is trapped inside the compacted powder body. Gas bubble voids form within the expanding body of semi-solid metal and are retained during solidification. This process results in a lightweight structure with a high degree of closed cell porosity. Metal foam parts can be produced to net shape in several different configurations.

The density of the metal foams can be controlled by adjusting the content of the foaming agent and several other foaming parameters, such as temperature and heating rate. The most commonly used aluminum alloys for foaming are Al-Si, 2xxx series, and 6xxx series Al alloys. The P/M approach as developed by Fraunhofer, however, can also be used for other metals including steel, lead, tin, zinc, brass, and bronze.

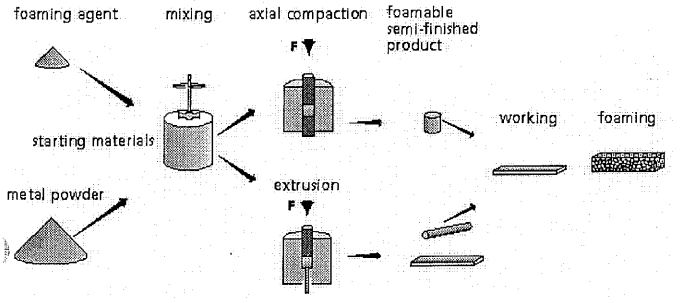


**Figure 1. Schematic diagram of Fraunhofer powder metallurgy process for producing porous metal foams**

## FABRICATION OF METAL FOAM COMPONENTS

### 3-Dimensional molded parts

Metal foams can be produced in several different configurations. Complex 3-dimensional metal foam parts can be molded to net-shape. The foamable preform of consolidated metal powder + foaming agent is placed inside the cavity of a forming tool. This mold assembly is then placed inside a furnace and heated to near the melting point of the metal alloy powder. The action of the foaming agent causes significant volume expansion resulting from the evolution of gas bubbles, which form the closed-cell pores. The molded foam part expands to fill the entire mold cavity, resulting in a 3-D shape. Figure 2 shows an aluminum foam part produced in a mold to replicate a shape that resembles a barbell weight. This part has a bulk density of approximately 0.5 g/cm$^3$, which corresponds to about 80 vol % porosity. A thin skin of relatively dense aluminum, approximately 0.5 – 1 mm thick, forms on the outer surface of the part.

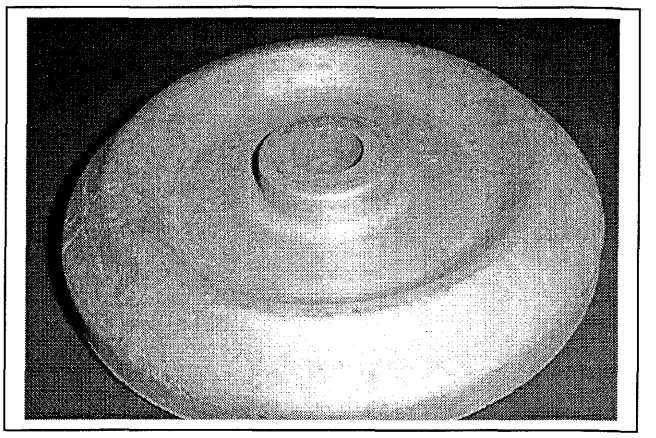

**Figure 2. Three-dimensional aluminum foam part molded to net shape in tooling. Thin metal skin on outer surface covers the inner foam core.**

### Aluminum foam sandwich panels

Sandwich panels of metal foam cores inside metal face sheets can also be produced. Aluminum foam sandwich panels, such as that shown in Figure 3, are being used by Karmann GmbH, a specialty designer and builder of convertible auto bodies, to develop AFS panels for automotive applications. Karmann has shown the high specific stiffness and weight reduction advantages of aluminum foam sandwich (AFS) panels in convertible body structures. These foam sandwich panels are formed by roll cladding aluminum face sheets onto an extruded billet of aluminum + foaming agent. The resulting preform sheet, consisting of the densified powder core sandwiched between aluminum face sheets, is heated to activate the foaming agent. This results in expansion of the foam core thickness by about 400%, yielding 80 vol% porosity.

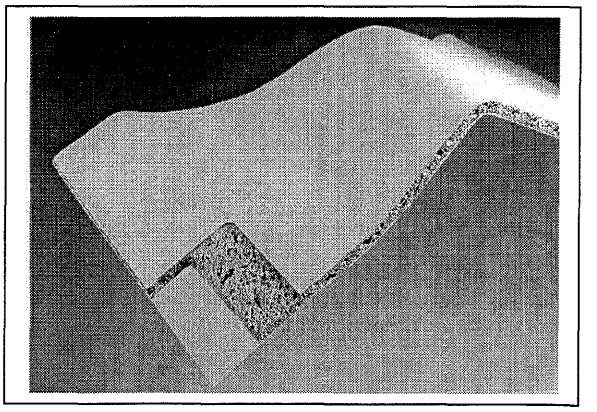

**Figure 3. Aluminum foam sandwich panel cold press-formed into contoured surface before foaming.**

Metal foam-filled tubes

Metal tubes or hollow profiles filled with metal foam have been produced out of aluminum, as shown in Figure 4. These Al foam-filled tubes were fabricated by inserting consolidated powder preforms into the hollow tubes and then heating to initiate the foaming reaction, thus filling the inside of the tubes with lightweight foam. In this case, the Al foams are metallurgically bonded to the inner surface of the tubes, providing an excellent interfacial bond. Foam-filled tubes provide significant stiffening, resistance to buckling, and ability to absorb crash energy.

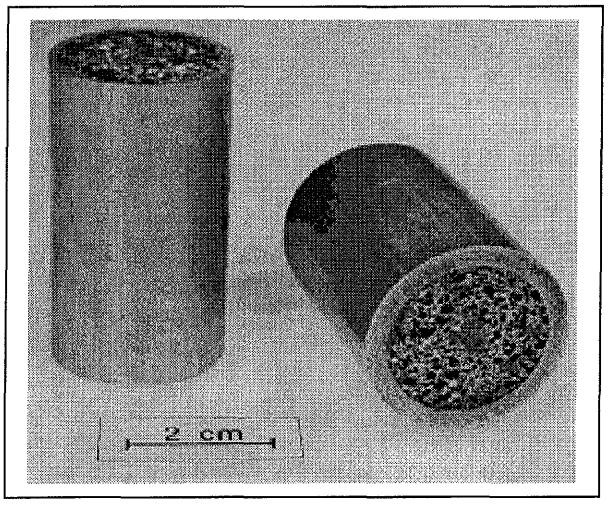


**Figure 4. Aluminum foams of Al-6Si-4Cu metallurgically bonded inside 6061 Al tubes.**

Alternatively, foam cores that have been formed separately can be inserted inside hollow tubes. This type of foam core may be either force fit into the tube or adhesively bonded to the tube ID surface. The foam can also be selectively located at critical high-load regions of the tubes. Tubular shapes with aluminum foam cores can also be hydroformed prior to the foaming step to create complex structures for specific applications.

## CHARACTERISTICS OF METAL FOAMS

Ultra-lightweight aluminum foams possess unique microstructural characteristics and physical properties that make them attractive for automotive, as well as other applications:

- Ultra-lightweight materials with high degree of homogeneous closed-cell porosity
- Foam microstructures tailorable over the range 40 to 80% porosity.
- High stiffness-to-weight and strength-to-weight ratios
- Ability to absorb energy from impact, crash, and explosive blasts
- Vibration damping and sound absorption
- Fire resistance and thermal insulating properties
- Metal foams are readily recycled

## SELECTED PROPERTIES OF ALUMINUM FOAMS

### COMPRESSIVE DEFORMATION BEHAVIOR

One of the most significant attributes of metal foams is their characteristic non-linear deformation behavior. This attribute lends itself to applications in which both lightweight construction and efficient absorption of deformation energy are important. In automotive applications, the crush energy absorption behavior of metal foams due to high strain rate deformation is important in designing vehicles for optimum crashworthiness.

Typical foam behavior in compressive loading

When subjected to uniaxial compressive loading, metal foams exhibit deformation behavior very similar to that of polymer foams. Three regions of compressive deformation are observed with metal foams, as depicted in Figure 5. In Region 1, the metal foam shows linear elastic deformation related to bending of the cell walls. In Region 2, the foam begins to undergo plastic deformation due to cell wall buckling. The initial wall buckling events result in the slight drop in stress observed at the transition between Regions 1 and 2. In this region, the compressive stress increases slightly as a function of strain. Region 3 is characterized by progressive collapse and crushing of cell walls. Significant densification of the foam occurs, resulting in a strong increase in stress with increasing compressive strain.

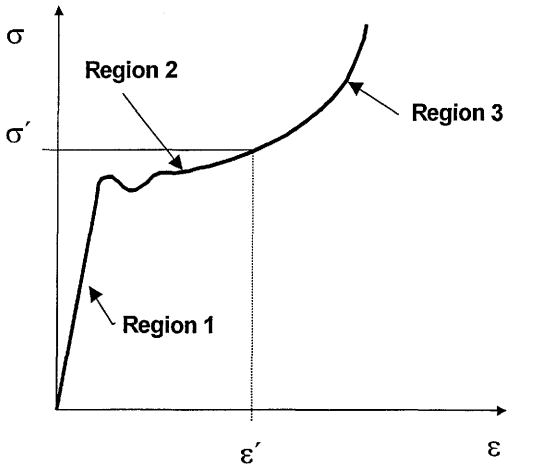


**Figure 5. Typical deformation behavior of metal foam under uniaxial compressive loading.**

Quasi-static compression testing

A study of the quasi-static and high strain rate behaviors of aluminum foams was conducted on Al 6061 foam. Foam plates 150 x 150 x 13 mm in size were fabricated with four different porosity levels ranging from 70 to 90 vol%. The nominal and relative densities of the four foam plates tested are presented in Table 1. Cylindrical test specimens 18 mm in diameter x 12 mm length were cut from the foam plates for both quasi-static and high strain rate compression tests. The cell size varied somewhat through the thickness and resulted, therefore, in a slight density gradient. Typical cell sizes were 4-5 mm in the interior of the plates and 2-3mm near to the external surfaces. Quasi-static compression tests were conducted using a displacement-controlled Instron test machine at a strain rate of $1.5x10^{-3}$ $s^{-1}$.

**Table 1. Densities of 6061 Aluminum Foam Plates Used in Quasi-static Compression Testing**

| Foam Plate No. | Density ($g/cm^3$) | Relative Density (%) |
|---|---|---|
| 1 | 0.34 | 12.6 |
| 2 | 0.47 | 17.4 |
| 3 | 0.57 | 21.1 |
| 4 | 0.82 | 30.4 |

The quasi-static compression stress-strain curves for the four different Al foam density levels are shown in Figure 6. The flow stress is clearly a strong function of the relative density of the foam. The experimental compressive stress-strain curves show the three distinct regions of deformation, as discussed earlier and shown schematically in Figure 5. Region 1 - linear elastic regime; Region 2 - cell collapse regime, in which the compressive stress increases slightly as a function of strain; and Region 3 - densification regime, in which the compressive stress increases rapidly as a function of strain. In Region 1, the deformation is only elastic and is caused by bending of the cell walls. This is followed by Region 2, in which the initial cell wall buckling events occur and the stress drops slightly. In Region 3, the foam collapses progressively in relatively weak locations and is gradually densified. The flow stress in the collapse region increased as the relative density increased, as expected, but the rate of densification was also higher in the denser samples. Strains in excess of 60% were easily achieved in all cases.

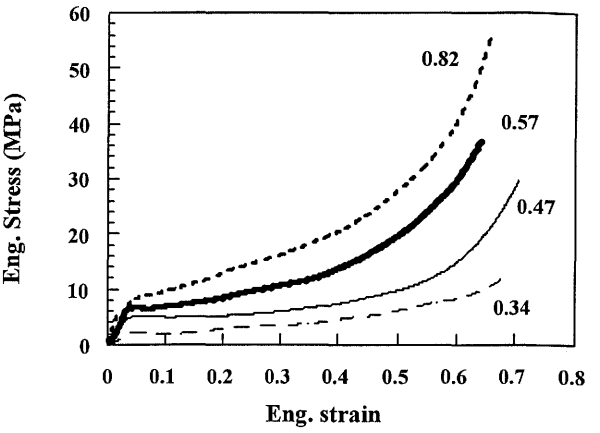


**Figure 6. Quasi-static compressive stress – strain curves for representative 6061 Al foam samples of each density.**

The increase in compressive flow stress with foam density for 6061 Al foams in this study is consistent with previous results obtained on Al-12Si alloy foams by Banhart et al. (5), as shown in Figure 7.

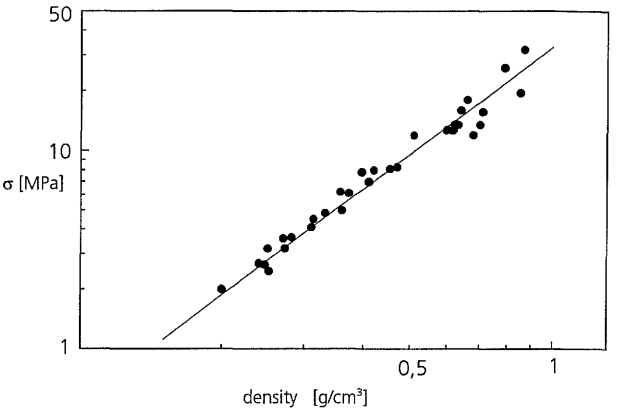


**Figure 7. Compression strength of Al-12Si foams as a function of density.**

Microscopic observations of compressive deformation

The sequence of deformation events during quasi-static compression testing of 6061 Al foam was recorded digitally. Figure 8 shows several of the frames of a typical montage of recorded images. The time in seconds at each frame is marked. The compressive loading axis was horizontal in this figure. Frame 1, at 0 sec, shows an undeformed region containing several cells at the beginning of the test. As soon as the compressive loading was initiated, the thinnest sections of cell walls approximately parallel to the compression axis started to buckle, as shown in the frame at 20 sec. In the later stages of deformation, frames at 90 sec and 120 s, the cell walls normal to the compression axis were torn due to the induced tensile strains. It was also observed that the deformation was highly non-homogeneous due to the statistical nature of the metal

foam microstructure. Feature "A" in Figure 8 shows an example of cell wall buckling, while Feature "B" shows tensile fracture of a cell wall. The cells to the left experienced essentially no deformation, while the adjacent cells were almost totally collapsed by the compressive loading.

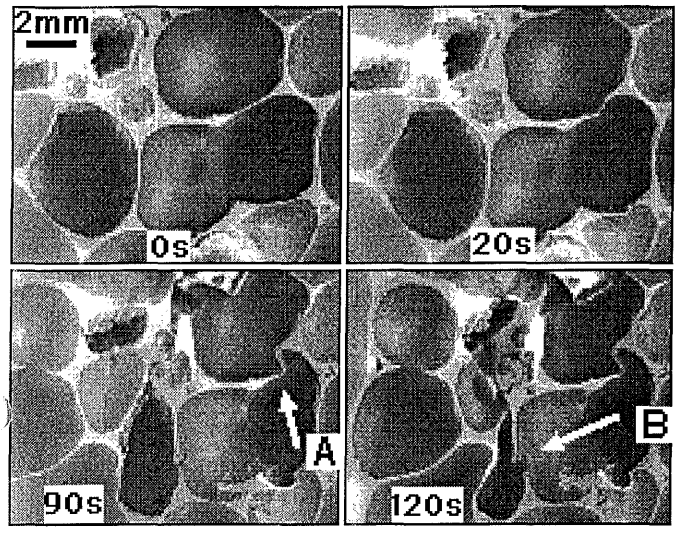


**Figure 8. Time-lapse sequence of photomicrographs showing inhomogeneous compressive deformation behavior of 6061 Al foam. Cell wall buckling (A) and tensile fracture (B).**

High-strain rate compression testing

The high strain rate testing was performed on a compression-type Split Hopkinson Pressure Bar (SHPB) apparatus. A schematic diagram of the SHPB test apparatus is shown in Figure 9. Details of the SHPB apparatus, testing procedures, and data analysis methodology have been presented elsewhere. (6) High strain rate tests were conducted on the Al foam specimens over the range of $3x10^2$ to $2x10^3$ $s^{-1}$. Briefly, in this technique a cylindrical specimen is mounted between the long incident and transmitter bars, while a shorter striker bar is used to impact to the end of the incident bar. This impact creates a compressive pulse which travels down the incident bar and into the specimen which then deforms as it is sandwiched between incident and transmitter bars. The strains measured by strain gages on the incident and transmitter bars are then used to determine strain rate, strain and stress in the specimen using one dimensional elastic wave analysis on the bars. High strain rate tests were conducted on the foam at strain rates up to ~$2.0x10^3s^{-1}$. The strain rates involved in automobiles during impact accidents are most frequently in the range between ~$1x10^2$ and ~$1x10^3$ $s^{-1}$ and the investigated strain rates are, therefore, relevant to impacts involved in such accidents.

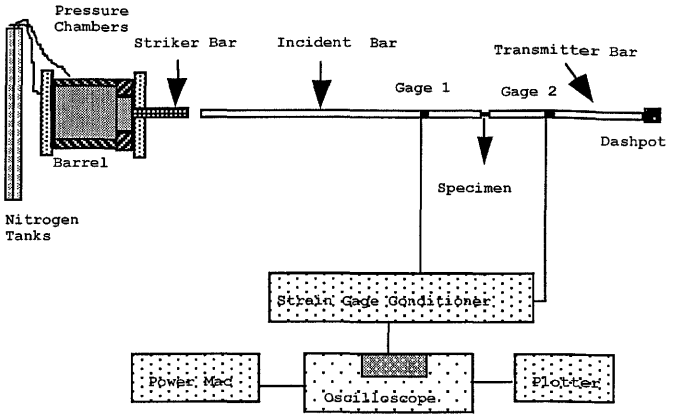


**Figure 9. Schematic diagram of Split Hopkinson Pressure Bar test apparatus.**

The same set of 6061 Al foams as were tested under quasi-static conditions were also tested at high strain rates in the SHPB apparatus. Figure 10 shows typical stress-strain curves for foams of three different densities tested at a strain rate of $2x10^3$ $s^{-1}$. Again, the flow stress values of the foam are seen to be a strong function of relative density although it is also noted that the areas under the stress strain curves, which scale with the energy absorbed, do not scale linearly with the density. The respective areas under the curves were calculated between 5% and 25% strain, the latter being the maximum strain obtainable at the lowest strain rate in the SHPB. These results are plotted as a function of density in Figure 14 and discussed in the next section on "Crash Energy Management".

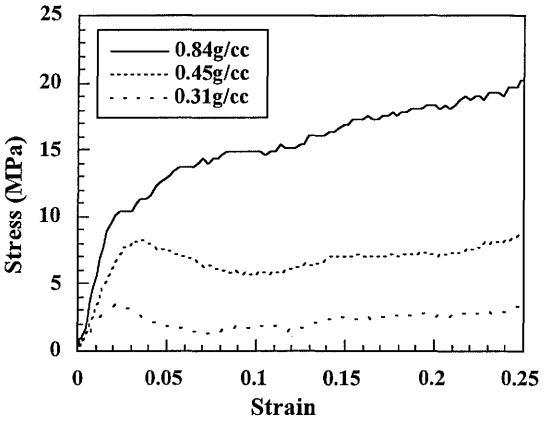


**Figure 10. High strain rate stress *vs.* strain curves at $2x10^3s^{-1}$ for Al foams of three different densities.**

To determine whether the Al foams exhibited a strain rate dependence, all the quasi-static and high strain rate test data were combined into one plot showing measured flow stress vs. foam density. The results are presented in Figure 11, in which data for four different strain rates from quasi-static up to $2x10^3$ $s^{-1}$ are indicated by different symbols. The scatter of the data

can be explained by factors other than strain rate, e.g. sample-to-sample variation in foam density and statistical distribution of pore sizes and shapes within samples of same nominal density. Thus, no clear evidence of any strain rate dependence was observed for compressive deformation of Al 6061 foams in this study.

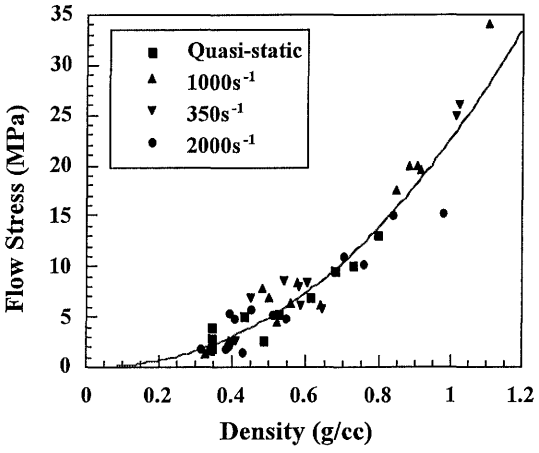


**Figure 11. Compressive strength data vs. foam density for all strain rates tested.**

## CRASH ENERGY MANAGEMENT

Metal foams offer great potential for applications in systems requiring crash energy absorption. The characteristic shape of metal foam compressive stress-strain curves, with a nearly constant plateau stress, allows absorption of large amounts of energy at a relatively low stress level.

Figure 12 schematically compares the typical energy absorption behavior of a fully dense elastic solid with that of a porous metal foam. The foam can absorb much more energy than the dense solid for a specified peak stress level. (At a specified strain level, the dense solid can absorb more energy than foam, but this is not a realistic condition for practical crash energy management.)

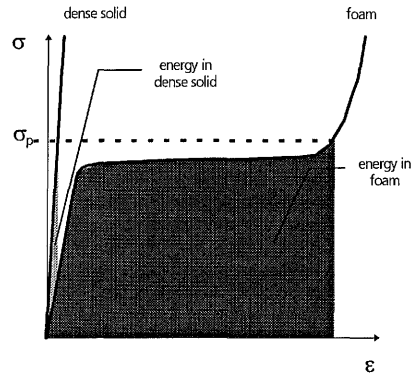


**Figure 12. Schematic diagram comparing energy absorption behavior via compressive deformation for foam and dense solid.**

Figure 13 shows the experimental test data on Al foams with three density levels: 0.31 g/cm$^3$ (12% fractional density), 0.45 g/cm$^3$ (17% fractional density) and 0.70 g/cm$^3$ (26% fractional density). The shaded areas represent the equivalent amounts of absorbed energy. In this case, the foam in the medium density range absorbs the given amount of energy at the lowest stress level. Thus, for a given energy absorption requirement and maximum allowable peak stress, the foam density can be tailored to the situation.

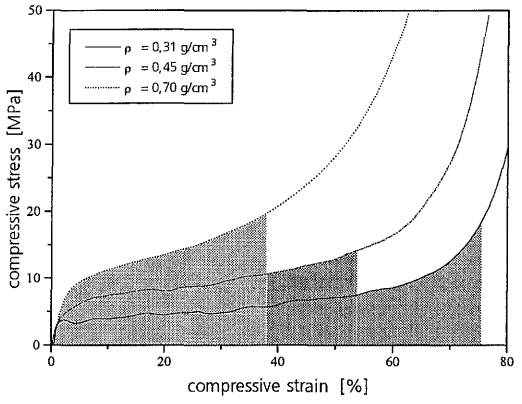


**Figure 13. Compressive stress-strain curves for Al foams at three different density levels. Shaded areas under each curve represent equivalent amounts of absorbed energy.**

The effect of metal foam density on relative energy absorption capability is shown in Figure 14 for the 6061 Al foam materials described above in quasi-static and high strain rate testing. As indicated in this figure, the amount of energy absorbed between 5 and 25% strain increased by a factor of 7X for an increase in foam density from 0.31 g/cm$^3$ to 0.84 g/cm$^3$.

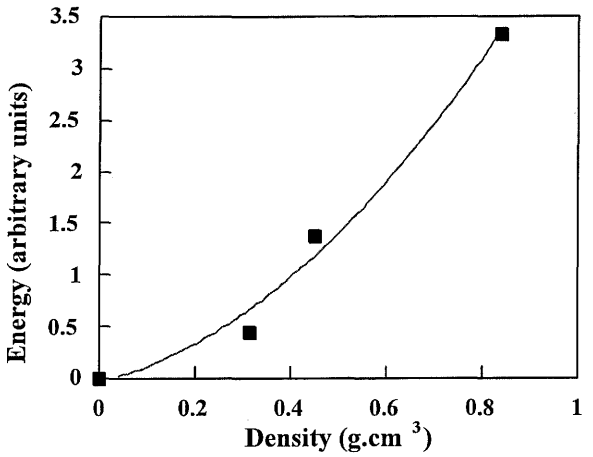


**Figure 14. Relative amounts of energy absorbed during compression of 6061 Al foams between 5 and 25% strain as a function of foam density. (Arbitrary units).**

Figure 15 shows a compilation of data on energy absorption capability per unit volume for a broad array of metal foam materials and foam densities. These results again show the ability to tailor engineer aluminum foams for specific application requirements.

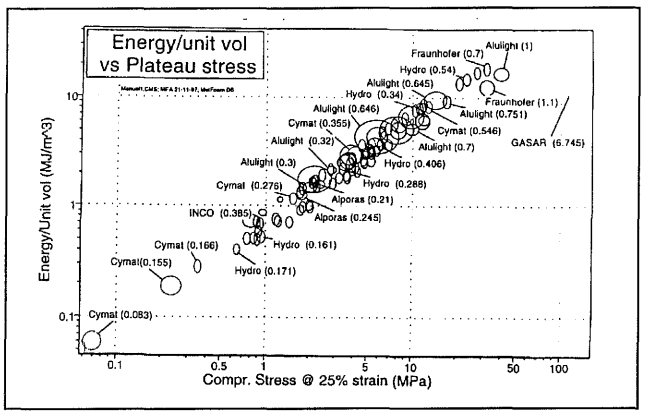


**Figure 15. Energy absorption per unit volume for a broad range of metal foam materials and densities. Foam density in g/cm$^3$ is shown in parentheses.**

## ELASTIC BEHAVIOR

A knowledge of the elastic properties of metal foams is required in order to properly design components for engineered structures. The elastic modulus of Al-12Si alloy was measured as a function of density by Banhart using the resonance frequency method (7). Figure 16 shows the results of elastic modulus vs. density over the range 0.5 g/cm$^3$ to 2.65 g/cm$^3$ (fully dense foamable precursor).

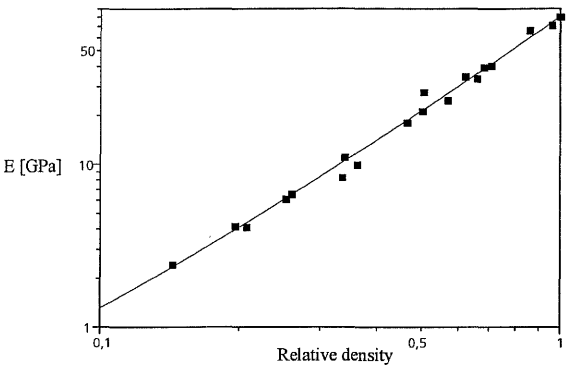


**Figure 16. Elastic modulus of Al-12Si foams as a function of density.**

## BENDING OF FOAM-FILLED TUBES

Another attractive characteristic of Al foams is their ability to stiffen structural members and potentially reduce overall system weight. The advantage of using lightweight Al foam fillers inside steel tubes to increase their resistance to bending has been demonstrated. Inserts of Al-7Si alloy foam were produced by in-situ foaming inside rectangular tubes of low carbon steel (Type St37). The steel tubes had a hollow square cross-section of 50 mm x 50 mm x 1.5 mm wall and were 450 mm long. A test matrix of specimens of Al foam-filled steel tubes were fabricated with varying Al foam density and Al foam insert length. Columns with 450 mm Al foam inserts were fabricated by placing Al-7Si foamable precursor inside the hollow steel tubes and closing the ends. The steel tube with Al foamable precursor was then placed into a furnace pre-heated to 700°C, where it was heated to cause the foaming reaction, then removed from the furnace and cooled. The shorter Al foam inserts were produced by foaming inside steel tubes, removing and cutting to selected lengths, then mechanically inserted into steel tubes that were pre-heat treated at 700°C to approximate the metallurgical conditions in the steel tubes that contained in-situ foamed Al inserts.

Details of the Al-7Si foam-filled steel tube test specimens are summarized in Table 2. The 450 mm-long foam-filled tubes were tested in 3-point bending using a 400 mm support span with 50 mm diameter lubricated cylindrical rolls at the support and loading points. The cross-head speed was 4 mm/min. The bending test results are shown in Figure 17. The Al foam inserts were observed to have a noticeable beneficial effect on increasing the bending resistance. The unfilled steel tube exhibited a maximum bending force of 11.7 kN. Use of Al foam inserts increased the maximum force to 16.5 kN, an increase of 40%. With the limited number of tests conducted to date, it is not possible to determine the effects of foam density and foam insert length on the bending behavior. Additional bending tests of both steel and aluminum tubes with Al foam inserts is in progress.

**Table 2. Description of 3-point bending test specimens of Al-7Si foam-filled carbon steel tubes.**

| Test | Type of Al-7Si foam filling | | Additional treatment |
|---|---|---|---|
| | Foam length | Foam density | |
| 1 | 450 mm | 0.42 g/cm$^3$ | None |
| 2 | 450 mm | 0.41 g/cm$^3$ | None |
| 3 | 450 mm | 0.54 g/cm$^3$ | None |
| 4 | 450 mm | 0.42 g/cm$^3$ | None |
| 5 | 100 mm | 0.55 g/cm$^3$ | * Note 1 |
| 6 | None | N/A | * Note 2 |

* Note 1: Heat treated 700 °C before inserting foam
* Note 2: Heat treated empty tube – control sample

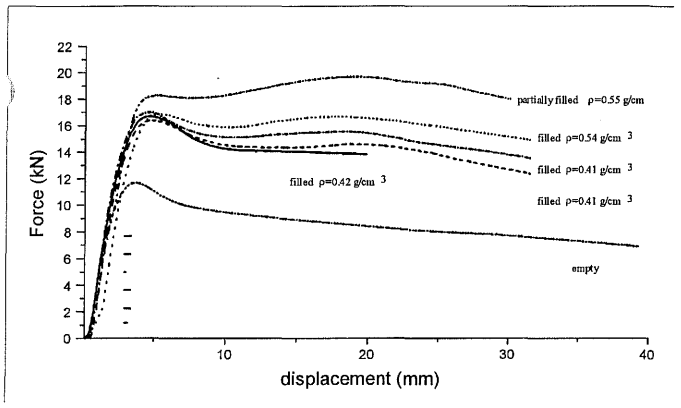


**Figure 17. Load vs. displacement curves for Al foam-filled steel tubes described in Table 2.**

## VIBRATION DAMPING

Control of vibration and NVH characteristics is very important for automotive applications. As the auto industry moves toward greater use of aluminum for weight reduction, this becomes even more critical due to the inferior vibration damping behavior of aluminum compared to steel and cast iron. Preliminary test results indicate that strategic use of aluminum foams can improve the damping characteristics of aluminum components.

The damping loss factor of Al-12Si foams has been measured as a function of foam density using a modified clamped cantilever test geometry. As indicated by the results shown in Figure 18, the damping capacity factor increases from a value of 15x10$^{-4}$ for dense unfoamed precursor material (density=2.55 g/cm$^3$) aluminum to about 25x10$^{-4}$ for Al-12Si foam with a density of 0.67 g/cm$^3$. The loss factor of the foams was not a smooth function of frequency over the investigated range of 100 to 1000 Hz, and no frequency dependence could be determined.

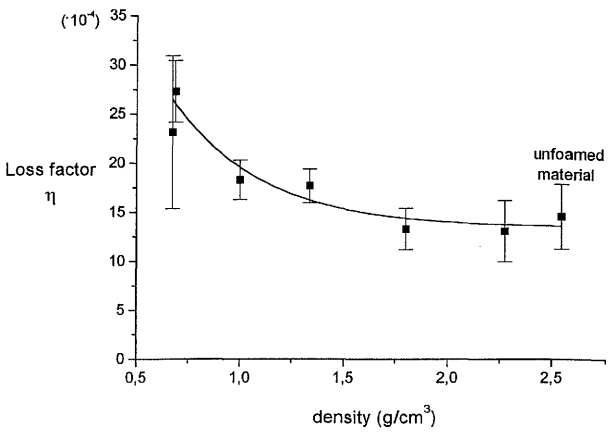


**Figure 18. Loss factor of a series of AlSi12 foams measured at 1kHz and room temperature.**

The damping behavior of aluminum foam sandwich panels has been studied by Karmann in collaboration with the Technical University of Dresden, Germany. The damping capacity of test panels of aluminum sheet, steel sheet, and aluminum foam sandwich (AFS) was measured over the frequency range of 100 to 500 Hz. As shown by the results in Figure 19, the aluminum foam sandwich panel showed significantly better damping behavior than either the aluminum or steel sheets, especially in the frequency range 50-400 Hz.

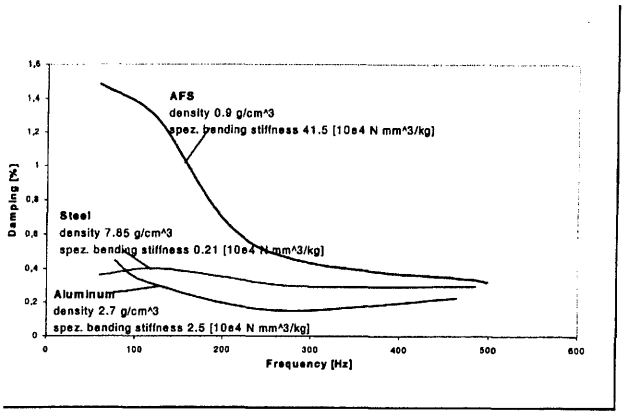


**Figure 19. Vibration damping measurements on aluminum foam sandwich (AFS) panels, compared with steel and aluminum sheet.**

## AUTOMOTIVE APPLICATIONS OF METAL FOAMS

The characteristics and materials properties exhibited by aluminum foams suggest numerous potential automotive applications of foam structures:

- Firewalls and rear kick-up panels
- Floor panels

- "A" and "B" pillars
- Energy absorbing bumpers
- Side-impact door intrusion bars
- Front crash rails
- Space frame components and roll bars
- Blast mitigation panels in military vehicles

Potential applications of metal foams include light weight cores for sandwich panels, shells and tubes where the foam can increase the resistance to local buckling, increase the impact resistance, and improve the energy absorbing capacity of the structure. This latter property offers potential uses in transportation applications where, for example, foam-filling of hollow sections in automotive components, such as door intrusion beams and side rails, may reduce damage and injuries resulting from impact accidents. For this type of application, aluminum foam is more suitable than polymeric foams, because it deforms plastically under impact and with essentially no spring back, preventing further damage. Other important advantages of using aluminum foams over polymeric foams include high fire resistance, insensitivity to cold / hot weather and humidity, and ease of recycling.

Impact accidents produce loading rates which are higher than those of static or quasi-static rates and which may significantly alter mechanical response of the materials. Therefore, in designing with metallic foams as energy absorbing fillers, mechanical properties are needed for strain rates corresponding to those created by impact events. Quasi-static mechanical behavior of metallic foams has been fairly extensively studied and reported, but data on high-strain rate mechanical behavior of these materials are, just becoming available.

The AFS panels developed by Fraunhofer and Karmann, as described earlier, consist of aluminum foam cores 11 mm thick, with a porosity of 80 - 90 vol%, metallurgically bonded to aluminum alloy face sheets, which are 1 mm thick. AFS panels can be produced in sizes up to about 3 ft wide x 5 ft long. Karmann has demonstrated the advantages of AFS panels in providing increased specific stiffness, resistance to bending and torsional stresses, and significant weight reduction by replacing steel body structures. By using AFS panels to replace a conventional stamped steel firewall, Karmann was able to achieve an 8X improvement in stiffness and 50% reduction in component weight. Karmann is also investigation use of aluminum foam parts in other components, such as rear luggage kick-up panels and floor boards.

With regard to energy absorption, it is possible to engineer a controlled deformation into the crash zone of cars and trains with maximum impact energy dissipation. Possible applications include elements for side and front impact protection. Metal foam-filled hollow profiles present interesting deformation behavior and failure mode during buckling. In general, foam filling leads to higher deformation forces when profiles are bent and to higher energy absorption when profiles are axially crushed. Potential applications can be in bumpers, underside protection of trucks, A- and B- pillars, or other elements subjected to buckling or large deformation.

Sound absorption and heat insulation are also important properties in the automotive industry. In many cases, sound-absorbing elements must also be heat resistant. Existing polymer foams or a combination of materials, such as polymer foams and aluminum sheets, may not be desirable due to their poor heat resistance and recyclability. Elements incorporating aluminum foam may improve these properties to meet the design criteria.

## CONCLUSION

Metal foams based on a powder metallurgy process are a newly emerging class of ultra-lightweight engineering materials. This process can produce a broad range of metal alloy foams having a relatively homogeneous and isotropic pore structure. Metal foams can be fabricated into a variety of shapes including complex 3-D parts molded to net shape, foam sandwich panels with outer face sheets, and foam filled tubes or hydroformed shapes. Metallic foam made by this approach has a high fraction of porosity and exhibits a closed-cell microstructure. Aluminum foams provide very high specific stiffness and strength, high crush energy absorption capability, shock wave attenuation, vibration damping, and thermal and sound insulation. Metal foams are particularly attractive for applications requiring high specific stiffness and energy absorption capabilities. Light, stiff structures made of aluminum foam and foam sandwich panels can help reduce vehicle weight, increase stiffness, and enhance crashworthiness and passenger safety.

## ACKNOWLEDGMENT

The authors wish to acknowledge the U.S. Army Research Office for support of the quasi-static and high strain rate testing.

## CONTACT

Dr. T. Dennis Claar
Fraunhofer Center - Delaware
501 Wyoming Road
Newark, DE 19716
Phone: 302-369-6721
Fax: 302-3696763
e-mail: dclaar@fraunhofer.org

## REFERENCES


1. J. Banhart and J. Baumeister, *Production Methods for Metallic Foams,* Porous and Cellular Materials for Structural Applications, MRS Symposium Proceedings, Vol. 521, 121 (1998).

2. J. Baumeister and H. Schrader, "Method for Manufacturing Foamable Metal Bodies", U.S. Patent No. 5,151,246.

3. C.J. Yu, H.H. Eifert, M. Knüwer, M. Weber, and J. Baumeister, *Investigation for the Selection of Foaming Agents to Produce Steel Foams*, Porous and Cellular Materials for Structural Applications, MRS Symposium Proceedings, Vol. 521, 145 (1998).

4. J. Banhart, J. Baumeister, M. Weber, *Powder Metallurgical Technology for the Production of Metal Foam,* Proc. European Conf. on Advanced PM Materials, Birmingham, p. 201 (Oct. 23 - 25, 1995).

5. J. Banhart, J. Baumeister: *Deformation Characteristics of Metal Foams*, J. Mat. Sci., **33**, 1431 (1998).

6. G. T. Gray III, *Methods in Materials Research*, (Wiley, New York, NY) 1997.

7. J. Banhart, J. Baumeister, and M. Weber, *Damping Properties of Aluminum Foams,* Materials Science and Engineering, A205, pp.221 (1996)